



Detection of anti-*Neospora* antibodies in bovine serum by using spiky Au–CdTe nanocomplexes

Hongjian Zhou^{a,1}, Jinhua Dong^{b,1}, Vipin Kumar Deo^b, Enoch Y. Park^{b,c,*}, Jaebeom Lee^{a,*}

^a Department of Nano Fusion Technology, Pusan National University, Miryang 627-706, Republic of Korea

^b Laboratory of Biotechnology, Graduate School of Science and Technology, Shizuoka University, Shizuoka 422-8529, Japan

^c Laboratory of Biotechnology, Department of Applied Biological Chemistry, Faculty of Agriculture, Shizuoka University, Shizuoka 422-8529, Japan

ARTICLE INFO

Article history:

Received 5 October 2012

Received in revised form 7 December 2012

Accepted 19 December 2012

Available online xxx

Keywords:

Neosporosis

Quantum dots (QD)

Spiky Au nanoprobles

Au-QDs sandwich immunoassay

Silkworm expression

ABSTRACT

Detecting biomolecules via nanotechnology has become increasingly important in veterinary science. Neosporosis is an infectious disease that primarily affects cattle and it is caused by the intracellular parasite *Neospora caninum*. This microorganism now appears to a major cause of abortion in dairy cattle worldwide. We report herein on a rapid, sensitive, and inexpensive qualitative approach for detecting neosporosis based on photoluminescence (PL) enhancement between quantum dots (CdTe nanoparticles) and a unique form of spiky Au nanoparticles (SNP). We prepared anti-bovine IgG functionalized-SNPs, and a conjugated structure between quantum dots (QDs) and recombinant *N. caninum* protein that was expressed by silkworms. They bound easily when their common complementary target, anti-*Neospora* antibodies (ANABs) in bovine serum, was present. Binding was monitored by the PL enhancement of CdTe nanoparticles (NPs) in the PL spectrum that resulted from localized surface plasmons resonance (LSPR) of SNPs. The fluorescence intensities for samples from infected and healthy cattle were compared, for which significant differences in intensity were observed. The SNP-QDs sandwich nanostructures remained in solution and its optical properties allowed it to be easily quantified by using fluorescence spectra. More than 52% emission enhancement on the surface of the SNPs was attained compared with the CdTe NPs and the results were reproducible. Furthermore, the biosensor was suited for qualitatively analyzing ANABs in blood serum. The ease of operation of this system and its generality offer specific advantages over other immunoassay methods.

© 2012 Elsevier B.V. All rights reserved.

1. Introduction

Neosporosis is an infectious disease that affects dogs, cattle, sheep, and under experimental conditions rodents, pigs, monkeys, and cats [1–5]. *Neospora caninum* is an obligate intracellular protozoan parasite and is a major cause of abortion in dairy cattle in many countries. Proteins that are displayed on the surface of this intracellular pathogen are believed to play critical roles in its infectivity. Several *N. caninum* parasite surface proteins have been reported. Surface-associated protein 1 (NcSAG1) and NcSAG1-related sequence 2 (NcSRS2) are major surface proteins of *N. caninum*, and their antigenicity has also been documented [6,7]. The diagnosis of neosporosis by detecting anti-*Neospora* antibodies (ANABs) in bovine serum might be fast and practical [6,7]. For instance, an immunoperoxidase test that involves using specific

antibodies can be employed to identify *N. caninum* in tissue sections or biopsy specimens. Alternatively, an indirect fluorescent antibody test and several ELISAs can be used to detect antibodies [8,9]. Even though a large number of bioassays are available nowadays, only one has been commercialized using an ELISA kit by Boehringer Ingelheim Svanova Inc. Therefore, it is still necessary to develop new detection methods that are rapid and highly selective to significantly improve the technology that is used for monitoring biological environments and in medical diagnostics [10].

Various bioreactor systems have been developed to mass-produce recombinant proteins that have biological sensor functions such as bio-probes that exhibit a high degree of specificity. Bacteria, especially *Escherichia coli*, are the most popular type of expression system, but are limited in terms of their poor capacity for modifying expression proteins and in many cases because the proteins that they express are in insoluble form [11]. Yeasts and insect cells are superior to bacteria since the proteins that they express can be glycosylated, which makes them more close to their native protein form. However, these protein production systems are costly. The silkworm *Bombyx mori* was first used by Maeda et al. [12] to produce human α -interferon and is now used as a bioreactor to

* Corresponding authors.

E-mail addresses: acypark@ipc.shizuoka.ac.jp (E.Y. Park), jaebeom@pusan.ac.kr (J. Lee).

¹ These two authors contributed equally to this work.

produce many types of eukaryotic proteins that can be used for pharmaceutical purposes. In particular, an improved bacmid system, BmDH10Bac *CP-Chi*⁻, can be used to express proteins in the milligram range in larvae [13].

Over the past 2 decades, Au nanoparticles (NPs) have attracted increasing attention because of their unique nano-optical properties. These include surface plasmon bands (SPB), surface-enhanced Raman scattering (SERS), and Rayleigh resonance scattering (RRS), and they are well documented. Efficient coating with biomolecules via various interactions enables Au NPs to act as signal transducers in biorecognition binding applications [14,15]. Moreover, in the proximity of a metallic surface the fluorescence emissions of molecules can be enhanced by localized surface plasmons resonance (LSPR) of metallic NPs. This is also the case for metallic nanostructures and NPs that are adjacent to quantum dots [16–19]. In noble metallic NPs, LSPR presents strong absorption and scattering cross-section and is sensitive to the local refractive index, size, shape, and chemical compositions of the nanostructures [20]. The presence of adjunct metallic nanoparticles not only enhances the fluorescence intensity but also stabilizes quantum dots against photo-bleaching, which further enhances their practical uses in bioimaging and biosensor applications [21]. For example, Ciftja et al. presented an updated review on the metal enhancement of fluorescence (MEF) of semiconductor, silicon and carbon quantum dots (QDs) that is achieved with LSPR [22]. Moreover, he also anticipated that the QDs/metal nanocomposites that can be dispersed in an aqueous solvent would be particularly suitable for the development of new bioanalytical methodologies where sensitivity and selectivity are the critical factor. Lin et al. studied that photoluminescence enhancement of CdS NPs via surface plasmon mode coupling, CdS-conjugated Ag nanoplates by forward–reverse cation exchange method for the application of cell imaging [23]. Oh et al. reported an inhibition assay method based on the modulation in fluorescence resonance energy transfer (FRET) efficiency between QDs and spherical Au NPs in the presence of the streptavidin–biotin that inhibit the interaction between QDs- and Au NP-conjugated biomolecules [24].

Recently, with the development of nanotechnology, researchers have been pushing the envelope to expand the applications of NPs with unique properties to construct novel receptor such as quantum dots, carbon nanotubes, nanowires, and magnetic NPs. However, the application of such receptor structure is often limited by their solubility and stability, requirements for expensive instruments, and most importantly, their uncontrollable responses to complex biological samples. Generally, practical sensors must work to minimize the complexity of the system. Therefore, it is a big challenge to detect proteins in real media by using newly developed detection platforms in clinical applications. Metal nanostructures, especially rough metallic nanostructures, exhibit remarkable optical properties due to the excitation of their surface plasmons by incident light, which significantly enhances the electromagnetic field at the nanoparticle surface [25]. Therefore, utilizing rough-surface metallic nanostructures that enhance quantum dot fluorescence may ultimately provide practical routes for enhancing light emission from a variety of materials systems and devices far beyond specific applications to bioimaging and biosensors.

In this study, we examined the properties of spiky Au-NPs (SNPs), which are three-dimensionally branched NPs that have more than 20 epitaxially grown tips and exhibit high yields and narrow size distributions at room temperature. We demonstrated a proof of concept of using SNP–CdTe NPs conjugation as a novel fluorescence-sensor platform for detecting proteins. To the best of our knowledge, despite a number of bioanalytical applications of NPs [25], this work is unique in terms of optical and biological properties because it involves enhancing the fluorescence of QDs by LSPR of rough-surfaced metallic NPs. In addition, it

uses recombinant proteins that are expressed by silkworms for immunoassay to develop an alert system for monitoring veterinary diseases. Antibody detection was accomplished as follows: anti-bovine IgG functionalized SNPs were bound to a complementary target (ANABs) in bovine serum. To achieve high sensitivity, recombinant *N. caninum* protein-conjugated quantum dots (rNcSAG1- or rNcSRS2–CdTe NPs) were employed to produce a fluorescence signal. Significant differences in intensity were observed between serum samples from infected and healthy cattle, which resulted from enhanced fluorescence of the Au-QD sandwich nanocomplex with its target proteins.

2. Experimental details

2.1. Spiky Au nanoparticle synthesis

All of the chemicals that we used were purchased from Sigma–Aldrich or Wako Pure Chemical Industries, Ltd. (Osaka, Japan) and used as received. Ultrapure Millipore water (>18.2 MΩ) was used as a solvent. All the glassware were cleaned with aqua regia (HCl/HNO₃ at a 3:1 ratio by volume) and rinsed with ethanol and ultrapure water (*Caution! Aqua regia is a very corrosive oxidizing agent that should be handled with great care*). The spiky Au NPs were synthesized by reducing HAuCl₄ with 4-(2-hydroxyethyl)-1-piperazineethane-sulfonic acid (HEPES) and stabilized according to Wang's method [26] with slight modifications. An aqueous stock solution of 100 mM HEPES was prepared with ultrapure water and its pH was adjusted to 7.4 at 25 °C by adding 1 M NaOH. In a typical experiment to synthesize SNPs, 1 mL of 100 mM HEPES (pH 7.4) was mixed with 9 mL of deionized water followed by the addition of 250 μL of 20 mM HAuCl₄. Without shaking, the color of the solution changed from light yellow to pink and finally to turbid blue at room temperature within 30 min.

2.2. Synthesizing thiol-capped CdTe NPs

CdTe NPs were synthesized as described previously [27]. Briefly, 0.985 g (2.35 mmol) of Cd(ClO₄)₂·6H₂O was dissolved in 125 mL of water, and 5.7 mmol of thioglycolic acid (TGA) was added under stirring. The pH was adjusted to the appropriate value (11.4–11.6) by adding 1 M NaOH dropwise. The solution was placed in a three-necked flask and deaerated by bubbling in N₂ for 30 min. Under stirring, H₂Te gas that was generated by the reaction of 0.2 g (0.46 mmol) of Al₂Te₃ lumps with 15–20 mL of 0.5 M H₂SO₄ in the N₂ atmosphere was passed through the solution together with slowly flowing nitrogen for 20 min. The CdTe precursors that were formed were converted into CdTe nanocrystals by refluxing the reaction mixture at 100 °C under open air for 20 min with a condenser that was attached to the apparatus.

2.3. Preparing goat anti-bovine IgG conjugated SNP nanoprobe

The SNPs were first modified with 8-mercaptooctanoic acid (MA) by adding 1.0 mL of MA to 9.0 mL of SNPs to reach a final concentration of 0.5 mM. A self-assembled monolayer (SAM) on the gold surface was formed after incubating the mixture overnight with gentle shaking at room temperature. Next, the mixture was centrifuged (4000 rpm for 15 min at 4 °C). The supernatant was decanted and the pellet was rinsed with PBS (0.01 M at pH 7.4). This centrifuging/resuspending step was repeated more than 3 times to remove the unbound MA molecules. The final carboxyl-stabilized Au NPs were concentrated to 5.0 mL. Subsequently, 100 μL of 0.1 M *N*-hydroxysuccinimide (NHS) was immediately added after activating it with 400 μL of 0.1 M 1-ethyl-3-(3-dimethylaminopropyl) carbodiimide (EDC) solution, and the mixture was incubated for 10 min. Afterwards, the goat anti-bovine IgG detection probe was

added to the solution to reach a final concentration of 0.5 μM . The mixed solution was incubated for 8 h at room temperature with gentle shaking and the centrifuging/rinsing procedure was repeated three times to remove the unbound goat anti-bovine IgG detection probe. The final pellet was suspended in 5.0 mL of PBS buffer solution (0.01 M, pH 7.4) and stored at 4 °C for further use.

2.4. Expressing and purifying rNcSAG1 and rNcSRS2

The recombinant *N. caninum* proteins, rNcSAG1 and rNcSRS2 were expressed in silkworms by using a bacmid protein expression system and purified with an anti-FLAG affinity resin as described by Dong et al. [28] and Otsuki et al. [29]. As shown in Fig. S1 of supplementary information, the rNcSAG1 and rNcSRS2 genes were amplified by using the genomic DNA of *N. caninum* strain Nc-1 (ATCC no. 50843) by the polymerase chain reaction (PCR) and cloned into a pENTR/TOPO plasmid (Invitrogen, USA) by employing the topoisomerase reaction. Using this plasmid, we inserted full-length rNcSAG1 or rNcSRS2 genes into pDEST8 by using Gateway technology (Invitrogen, USA) to construct plasmid pDEST-rNcSAG1 or pDEST-rNcSRS2, which were then used to transform *E. coli* BmDH10Bac CP-*Chi*⁻ [13]. *E. coli* colonies that contained recombinant *B. mori* nucleopolyhedron virus bacmid (rBmNPV-rNcSAG1 or rBmNPV-rNcSRS2) were identified by blue-white selection: the white colonies were deemed to harbor recombinant bacmids. PCR was used to confirm the presence of the target genes. rBmNPV-rNcSAG1 or rBmNPV-rNcSRS2 was then extracted from a large-scale culture of recombinant *E. coli* and used to express the respective protein in silkworms.

The silkworms expressed biologically active protein that was functionally similar to the native protein because they carried out post-translational modifications, including glycosylation. The recombinant bacmid rBmNPV-rNcSAG1 or rBmNPV-rNcSRS2 (10 μg each) was mixed with one-tenth volume of DMRIE-C (Invitrogen, USA) and incubated at room temperature for over 45 min. Each silkworm on the first day of the fifth instars larvae (Ehime Sansyu Co. Ltd., Ehime, Japan) was injected with 50 μL of the mixture and reared for 5–7 days, after which its hemolymph was collected. Recombinant protein rNcSAG1 or rNcSRS2 was purified from the silkworm larval hemolymph by using anti-FLAG M2 Affinity Gel (Sigma, USA), according to the instructions that were provided by the manufacturer. It was then conjugated with QDs and the product was used to detect anti-rNcSAG1 or anti-SRS2 antibodies in the sera of *N. caninum*-infected cattle.

2.5. Preparation of rNcSAG1- or rNcSRS2-captured CdTe nanoprobos

Pre-synthesized TGA-modified CdTe NPs were washed twice with ethanol. The CdTe NPs were centrifuged at 50,000 rpm for 1 h at 4 °C by using a micro-ultracentrifuge (Himac CS120GXII, Hitachi, Japan) to remove the extra free TGA. Subsequently, 100 μL of 0.1 M NHS was immediately added after it was activated with 400 μL of 0.1 M EDC and then it was incubated for 10 min. It was then conjugated with rNcSAG1 or rNcSRS2 by using the same protocol for goat anti-bovine IgG modified SNP nanoprobos. The mixture was incubated for 8 h at room temperature with gentle shaking, washed twice (50,000 rpm for 1 h at 4 °C), and stored in a 1.0 mL PBS solution at 4 °C until further use.

2.6. Detecting antibodies in bovine serum by using SNP-CdTe nanocomposite

Fig. S2 (as shown in supplementary information) illustrates the SNP-CdTe nanocomposite that was used to detect ANABs in bovine serum. In a typical experiment, 200 μL of SNP nanoprobos that

had been modified by goat anti-bovine IgG were added to three micro-centrifuge tubes and then 1 μL of three different types of sample (control, negative, and positive) was added to these three micro-centrifuge tubes, respectively. The control sample was in PBS buffer, the negative sample was the serum of healthy cattle in which no anti-*Neospora* antibodies were present (denoted as negative serum), and the positive sample was the serum of *N. caninum*-infected cattle that contained the target antibodies ANABs (denoted as positive serum). The exact concentration of the ANABs in the serum that we analyzed was not known since our sensor system was used to directly monitor the non-purified serum from the neosporosis-infected cattle. Finally, 20 μL of CdTe NPs that were modified by rNcSAG1 or rNcSRS2 were added to the above samples and the samples were divided into two groups (rNcSAG1 and rNcSRS2). Nanocomposite sensor experiments were conducted more than 20 times from two batches of sera for each group to collect reproducible and confidential data. The mixture was incubated for 1 h at room temperature to ensure all of the target segments were recognized. Then, an infinite[®] F500 microplate fluorescence reader (TECAN, Japan) was employed to measure the differences in fluorescence intensity of the QDs probes that were used to detect different serums in the presence of SNPs for the SNP-rNcSAG1-CdTe and SNP-rNcSRS2-CdTe systems. The absorbances of the SNPs were measured using UV-vis spectroscopy (SCINCO, S310, Korea). The morphologies and sizes of the NPs were characterized using a high-resolution transmission electron microscope (HR-TEM, JEOL, JEM-3010, Japan). Their particle size distribution was monitored by Malvern zeta-sizer Nano S (Malvern Instruments Ltd., ZS Nano, UK) with a detection angle of 173°. All measurements in this study were taken at a temperature of 25 °C. The Nano S uses a 4 mW He-Ne laser operating at a wavelength of 633 nm. The intensity size distributions were obtained from analysis of the correction functions using the Multiple Narrow Modes algorithm in the instrument software. This algorithm is based upon a non-negative least squares fit. These intensity particle size distributions were converted into number using Mie theory.

3. Results and discussion

3.1. Characterizing protein-conjugated NPs

The quality of a self-assembled monolayer is crucial for nanoprobos, not only to maintain particle stability in highly strengthened ionic buffers but also to protect the surface from non-specific adsorption. MA was used as a linker between the bio-moiety and inorganic material to design a protein-sensor probe because of the excellent properties of the S-Au covalent bond. The MA-stabilized SNPs were conjugated with anti-bovine IgG by using one-pot EDC/NHS coupling. The UV-vis spectra of unmodified and anti-bovine IgG modified SNPs are shown in Fig. 1A. The unmodified SNPs in aqueous solution showed maximum absorption near 617 nm, which is a unique SNP plasmon band. Morphologically, SNPs are hybrids of spheres and branched particles [10,30,31]. According to the theoretical calculations of Hao et al. [32], Au tripods with a tip length of 27 nm exhibit plasmon resonance at \sim 700 nm. The hybridization of \sim 540 nm for spheres (\sim 66 nm) and \sim 700 nm for branched particles should result in plasmonic absorption peaks between these limits—the experimental value of \sim 617 nm for the SNPs fell within this range. After modifying the surface, the surface plasmon band of anti-bovine IgG modified SNPs was red-shifted and was observed at 630 nm. Furthermore, we measured the size distribution curve of SNP and anti-bovine IgG modified SNP which were shown in Fig. S5A and B of supplementary information. The results indicated that the size of SNP increased after modification by anti-bovine IgG. Fig. 1B shows PL spectra for

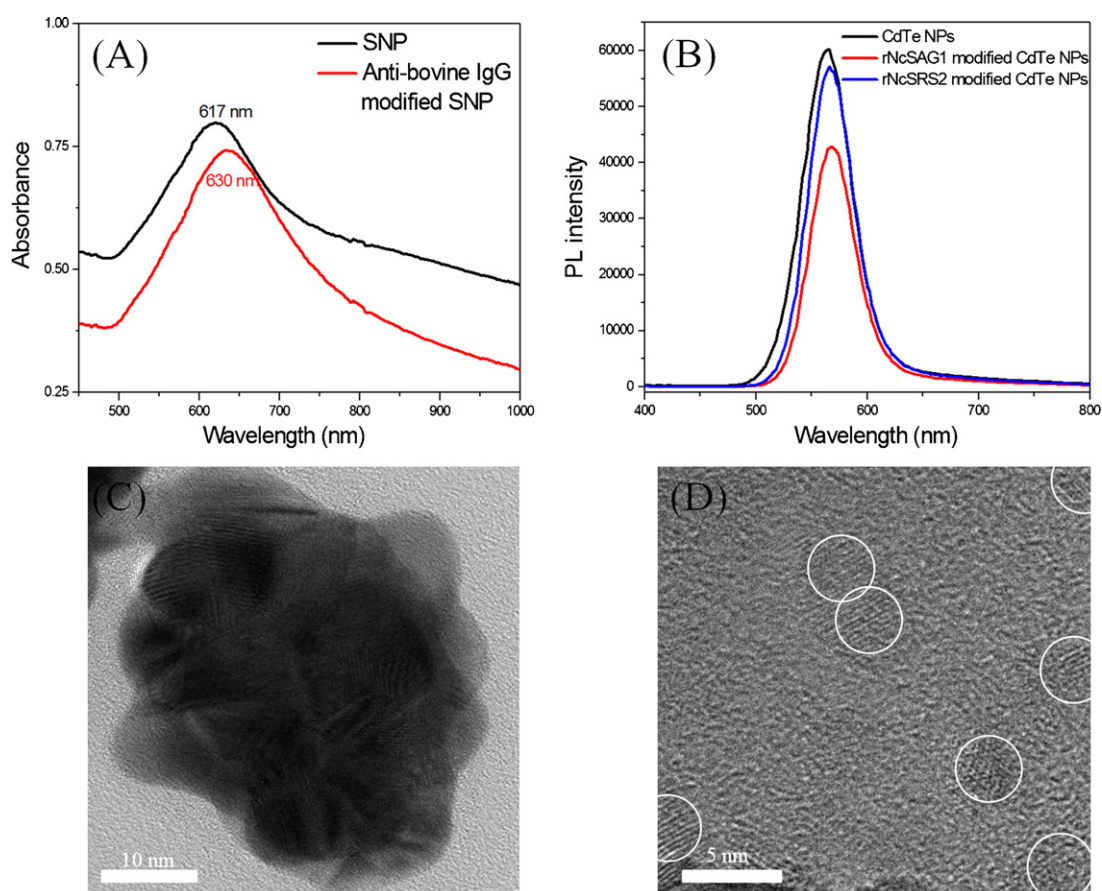


Fig. 1. (A) Comparison of UV-vis spectra for SNPs in aqueous solution and anti-bovine IgG modified SNPs in PBS solution. (B) Comparison of PL spectra for CdTe NPs in aqueous solution, and rNcSAG1 or rNcSRS2 modified CdTe nanoprobe in PBS solution. (C) TEM images of anti-bovine IgG modified SNPs and (D) TEM images of rNcSRS2 modified CdTe NPs.

the unmodified CdTe NPs, rNcSAG1-, and rNcSRS2-modified CdTe NPs. We observed that the maximum absorption of the unmodified CdTe NPs in aqueous solution was 563 nm. The PL spectra of the rNcSAG1 and rNcSRS2 modified CdTe NPs were slightly red shift, occurring at 568 and 566 nm, respectively. Their PL spectra and intensities had not broadened, nor were noticeably decreased. Concluding that the biological conjugation process on the CdTe NPs surface, had successfully occurred without any undue aggregation. Moreover, the size of modified CdTe NPs was also changed compared to the unmodified CdTe NPs (see in Fig. S5C–E).

On factor, detrimental for carrying out plasmon-induced PL enhancement, is the position of the plasmon and PL band [33]. In our nanocomposite design, >90% of the two bands had overlapped each other. SNP offer a great advantage, rather than using normal (small Au NPs), which generally exhibit a plasmon band near 520 nm. Fig. 1C and D shows TEM images of the SNPs and CdTe NPs after bioconjugation. The micrographs clearly show spiky Au NPs, about 50 nm in size, with approximately 20 branches per NP. The modified CdTe NPs were 5 nm in diameter on average. Therefore, results of UV-vis and PL spectra and TEM images suggests that the SNPs and CdTe NPs were readily modified by anti-bovine IgG, rNcSAG1, and rNcSRS2.

In order to further confirm the function of anti-bovine IgG modified SNP and rNcSAG1- and rNcSRS2-captured CdTe Nanoprobes, we performed enzyme-linked immunosorbent assay (ELISA) before detecting ANABs. Experimental details and ELISA results are shown in the supplementary information. As shown in Fig. S6A, higher signal was observed with anti-bovine IgG modified SNP than SNP, suggesting that anti-bovine IgG successfully modified SNP. The

rNcSAG1- and rNcSRS2-captured CdTe gave higher signal than the CdTe which was used as a control. This suggests that the rNcSAG1 or rNcSRS2 was successfully conjugated with CdTe NPs (Fig. S6B).

Each biologically conjugated NP was utilized to monitor the ANABs. Electron microscopic analysis was conducted to achieve a better insight on nanoscale clustering via an immunoassay of the nanomaterials. As can be seen in the high-resolution TEM images, the addition of rNcSAG1- and rNcSRS2-CdTe to the solution of anti-bovine IgG-SNP led to the formation of clusters in the positive serum (Fig. 2B and D). From these images, it is evident that the QDs and SNPs were close to each other due to the specific interaction between anti-bovine IgG, ANABs, and rNcSAG1 or rNcSRS2. This in turn, induced efficient PL enhancement of the QDs by the SNPs. In contrast, when the anti-bovine IgG-Au NPs were incubated with rNcSAG1- or rNcSRS2-CdTe in the negative serum, the formation of clusters between the QDs and Au NPs was negligible (Fig. 2A and C). This clearly supports the notion that externally added complementary target (ANABs) was conjugated with the QDs and SNPs and PL enhancement of the QDs owing to the LSPR of spiky Au NPs.

3.2. Detecting ANABs in bovine sera

The feasibility of using SNP-CdTe NPs nanocomposite as a fluorescence sensor platform for detecting ANABs was shown by using anti-bovine IgG, rNcSAG1, or rNcSRS2. The detection of ANABs could be translated by using the PL signal of the CdTe nanoprobe. When cattle are infected by *N. caninum*, they produce

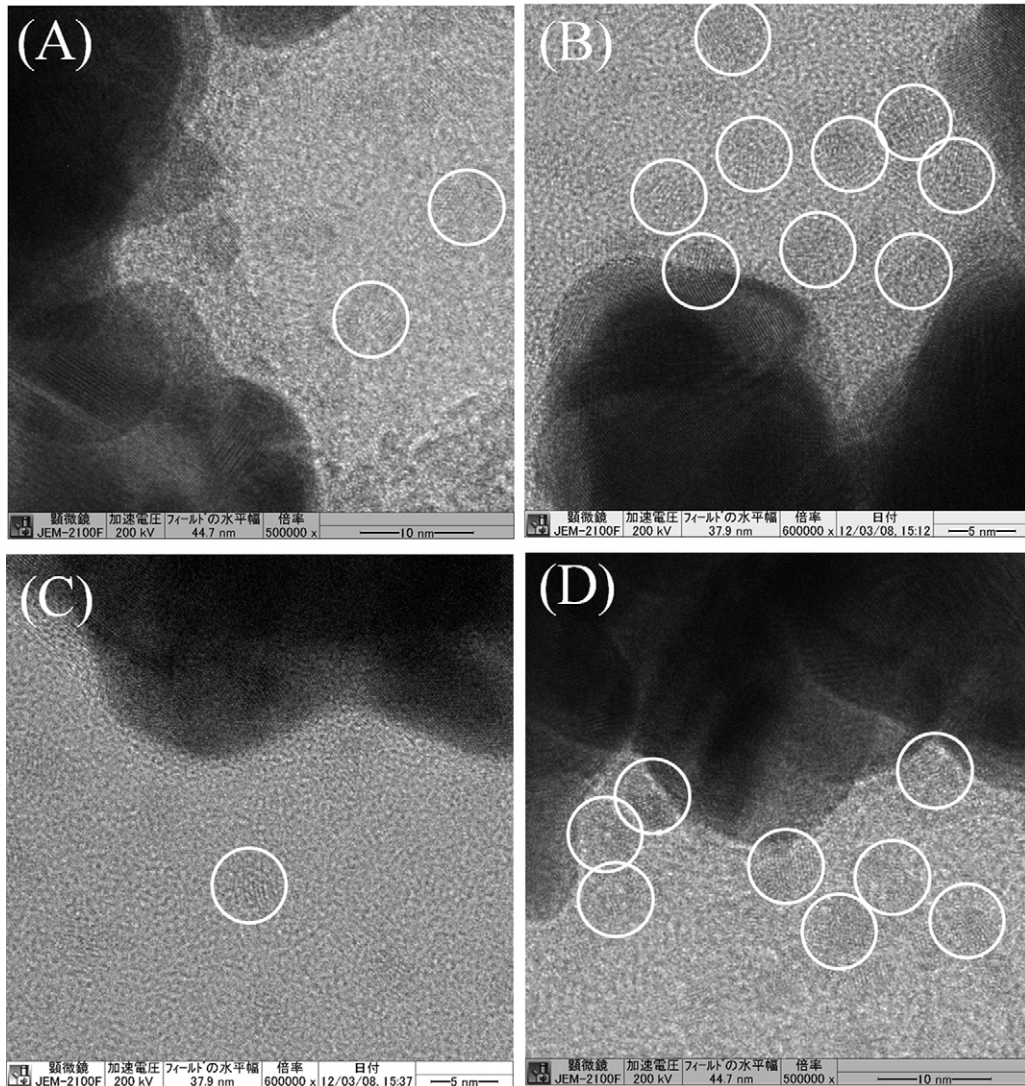


Fig. 2. TEM image of bioconjugation of CdTe NPs and SNPs by adding negative (A and C) and positive serum (B and D) to the Au-rNcSAG1–CdTe system (A and B) and Au-rNcSRS2–CdTe system (C and D). The CdTe NPs are outlined with guidelines (white circle).

anti-*N. caninum* antibodies. NcSAG1 and NcSRS2 are located on the surface of the *N. caninum* parasite and are highly antigenic [34–36]. Therefore, anti-NcSAG1 and anti-rNcSRS2 antibodies are produced by the adaptive immune system of cattle during the early stage of infection. By detecting the anti-NcSAG1 or anti-NcSRS2 antibodies through two nanocomposite sensor systems, we could recognize whether or not cattle are infected with *N. caninum*.

Fig. 3 shows the differences in the fluorescence intensity of the CdTe QDs probes for detecting different sera in the presence of SNPs by an infinite® F500 microplate fluorescence reader at SNP-rNcSAG1–CdTe and SNP-rNcSRS2–CdTe nanoprobe under excitation/emission wavelength of 485/535 nm. The $[(F/F_0) - 1]$ values showed that the PL difference that was generated by the sensor platform was directly related to the differentiation between the complementary and mismatched antibodies, where F_0 and F were the fluorescence intensities in the absence and presence of the target, respectively. Fig. 3A shows the results for the SNP-rNcSAG1–CdTe system. The PL intensity with PBS was detected to be $20,374 \pm 1287$ A.U., while with negative and positive serum sample, $23,019 \pm 1172$ A.U. and $26,769 \pm 1327$ A.U. were obtained. Compared with the control sample in PBS, the PL intensity

increased for the negative and positive serum samples. The fluorescence of CdTe was enhanced by about 31% ($p=0.0255$) by the addition of the positive serum while 13% ($p=0.0724$) enhancement was seen for the negative serum. Meanwhile, Fig. 3B shows the experimental results for the SNP-rNcSRS2–CdTe system. The PL intensity of CdTe in which PBS, negative and positive serum samples were added were $19,316 \pm 749$ A.U., $19,806 \pm 470$ A.U. and $29,450 \pm 749$ A.U., respectively. PL intensity with the positive serum sample was enhanced by 52% ($p=0.0036$) compared to the negative serum. However, the intensity of the negative serum was similar to that of the control sample to which PBS was added. This is because in the control and negative serum both the SNP and CdTe biosensor probes did not bind without anti-NcSRS2 antibodies, which resulted in the distance between the SNP and CdTe was not changed. However, in the presence of the positive serum, the anti-NcSRS2 antibodies bound to both the anti-bovine IgG modified SNP and rNcSRS2–CdTe, thereby permitting the appropriate distance to develop between the SNP and QDs. This in turn resulted in enhanced fluorescence emission. The distance between two NPs was considered to be approximately 20–30 nm since two whole IgG type antibodies were used in the immunoassay and the

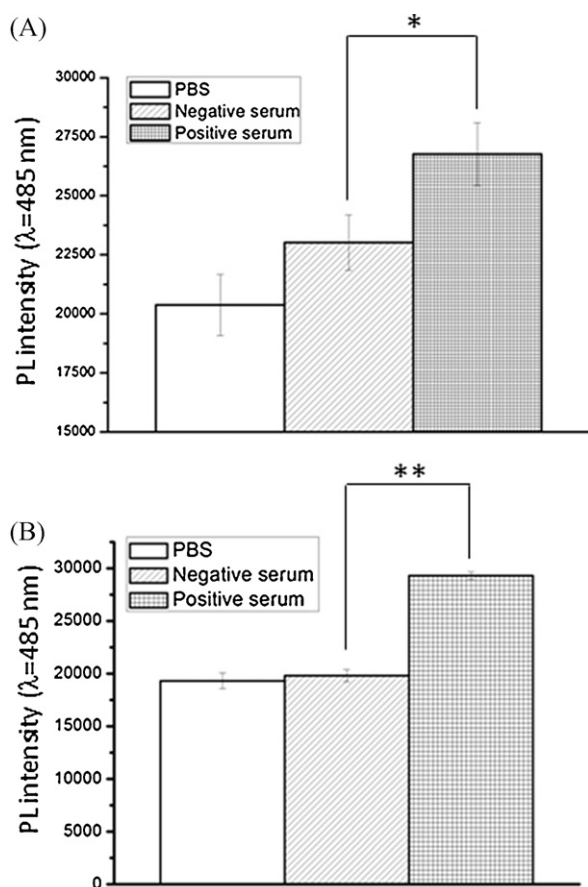


Fig. 3. Fluorescence intensities of CdTe NPs for detecting different sera (PBS, positive, and negative-serum) in the presence of SNPs under excitation/emission wavelengths of 485/535 nm that were produced by using an infinite® F500 microplate fluorescence reader. (A) SNP-rNcSAG1-CdTe system, (B) SNP-rNcSRS2-CdTe system, and (*) $p < 0.05$, (**) $p < 0.01$.

hydrodynamic diameter of IgG is 10–13 nm [37]. Over this range, PL enhancement or quenching can occur effectively between semiconductor and metallic NPs via dipole-dipole induced interactions [38]. Furthermore, in geometric terms, many tips on the spiky NPs possessed hot spots of plasmonic energy that enhanced the effects of adjacent semiconductor NPs [39]. Our results also indicated that anti-bovine IgG modified SNPs can strongly absorb complementary target protein (ANABs) and conjugate with rNcSRS2 modified CdTe NPs to enhance the fluorescence of CdTe NPs very effectively. The binding of rNcSAG1 and rNcSRS2 to the ANABs were also reported by Otsuki et al. with a traditional ELISA, and the results were very similar [29].

In this study, spiky Au NPs caused high plasmon-induced PL enhancement because of many plasmonic hot spots and a high coupling ratio (>90%) between the plasmonic band of SNP and the excitonic band of CdTe NPs. Coupling between excitons and plasmons is another crucial factor for obtaining efficient sensor devices because the coupling effect becomes stronger when the exciton energy is located closer to the plasmon peak. On the other hand, proteins play very important roles in detecting bio-moieties. Silkworm-expressed proteins are biologically active and most similar functionally to their native forms because of post-translational modifications, including glycosylation. Through these two specific optical and biological advantages, we constructed two systems for quickly detecting neosporosis in cattle by employing anti-bovine IgG modified spiky Au NPs and silkworm-recombinant *N. caninum* protein (rNcSAG1 or rNcSRS2). In contrast, in traditional assays such as ELISA, many steps such as blocking to decrease non-specific

signals, at least three washing steps after blocking, adding a primary antibody, and then sometimes a secondary antibody are necessary to detect anti-*N. caninum* antibodies. These types of assays are cumbersome and take more than 3 h. However, with our novel assay system, we do not need to perform washing steps, and our assay can be carried out quickly.

The results that were generated by our Au-rNcSAG1-CdTe system were similar to those of the Au-rNcSRS2-CdTe system. This suggests that in both systems, rNcSAG1 and rNcSRS2 on CdTe bound to their complementary antibody (anti-NcSAG1 antibody or anti-NcSRS2 antibody) steadfastly during consecutive self-assembly and bio-conjugation. Compared with the rNcSAG1 system, the rNcSRS2 system gave more ideal results i.e., higher enhancement and obvious optical discrimination with respect to the positive and negative samples. This is because rNcSRS2 may have resulted in a better response in the bovine immune system. Even though the concentration and volume of rNcSRS2-modified CdTe NPs was the same in the Au-rNcSRS2-CdTe system, the fluorescence of the free CdTe NPs was scarcely influenced by adding the negative serum in the absence of a target protein. It is likely that the Au-rNcSRS2-CdTe system may have exhibited more specificity than the Au-rNcSAG1-CdTe system. From these proof-of-concept results, the system that uses rNcSRS2 will be further developed as a biosensor system to minimize bio-moiety related variants.

All of the above observations suggest that both systems exhibited good reproducibility in distinguishing between complementary and mismatched target proteins. Even though we successfully identified neosporosis-positive sera by using these two systems, the increase in the PL intensity was still low compared with other advantageous conditions such as a high band overlapping ratio, geometrical uniqueness of the plasmonic NPs, and the high specificity of proteins that were produced by silkworms. For example, only 52% fluorescence enhancement was observed for the rNcSRS2 system. More factors should be examined to further enhance the fluorescence. The first factor that should be considered should be the distance between two NPs. In this study, the SNP and CdTe particles were linked by two antibodies (anti-bovine antibody and bovine anti-*Neospora* antibody) and they may have been separated by tens of nanometers. Even this distance enhanced the fluorescence signal enough to be able to detect the anti-*Neospora* antibodies in the sera. Thus, increased enhancement may be obtained by changing the distance between the particles. By employing biotechnological techniques, we also can make small antibody units such as fragments for antigen binding (Fab) that exhibit the same binding affinity as that of an antibody but are only half the molecular weight, or single chain variable regions (scFvs) that are only one-sixth the size of an antibody. In addition, the distance could be lengthened by adding a linker.

4. Conclusions

CdTe QD-SNP nanocomplexes were used successfully as a novel fluorescence-sensor platform for detecting designated proteins by immunoassay. SNPs are promising NPs in terms of being an effective universal sensor platform for fluorescence-enhanced detection because of their unique optical and geometrical properties. Both proteins, rNcSAG1 and rNcSRS2 that were expressed from silkworm were linked on CdTe QDs. Then, they were bound to their complementary antibody (anti-NcSAG1 antibody or anti-NcSRS2 antibody) steadfastly during consecutive self-assembly and bio-conjugation, resulting in higher enhancement and obvious optical discrimination with respect to the positive and negative samples. Therefore, since this sensing system is easy to operate, inexpensive, and versatile, with further study on quantitative analysis, it may be

incorporated into next generation protein detection tools that will be used to detect the early stages of the disease.

Acknowledgments

This work was partly supported by a Grant-in-Aid for Scientific Research (A) Grant No. 22248009 from the Ministry of Education, Culture, Sports, Science and Technology, Japan. It was also supported by a grant from the International Research and Development Program of the National Research Foundation of Korea funded by the Ministry of Education, Science and Technology of Korea; by the Financial Supporting Project of Long-term Overseas Dispatch of PNU's Tenure-track Faculty, 2012.

Appendix A. Supplementary data

Supplementary data associated with this article can be found, in the online version, at <http://dx.doi.org/10.1016/j.snb.2012.12.078>

References

- [1] I. Bjerkas, S.F. Mohn, J. Presthus, Unidentified cyst-forming sporozoon causing encephalomyelitis and myositis in dogs, *Parasitology Research* 70 (1984) 271–274.
- [2] D. Buxton, S.W. Maley, K.M. Thomson, A.J. Trees, E.A. Innes, Experimental infection of non-pregnant and pregnant sheep with *Neospora caninum*, *Journal of Comparative Pathology* 117 (1997) 1–16.
- [3] J.P. Dubey, A.N. Hamir, C.A. Hanlon, M.J. Topper, C.E. Rupprecht, Fatal necrotizing encephalitis in a raccoon associated with a Sarcocystis-like protozoon, *Journal of Veterinary Diagnostic Investigation* 2 (1990) 345–347.
- [4] D.S. Lindsay, N.S. Rippey, T.A. Powe, E.A. Sartin, J.P. Dubey, B.L. Blagburn, Abortions, fetal death, and stillbirths in pregnant pygmy goats inoculated with tachyzoites of *Neospora caninum*, *American Journal of Veterinary Research* 56 (1995) 1176.
- [5] S. Rojo-Montejo, E. Collantes-Fernandez, I. Lopez-Perez, V. Risco-Castillo, A. Prenafeta, L.M. Ortega-Mora, Evaluation of the protection conferred by a naturally attenuated *Neospora caninum* isolate against congenital and cerebral neosporosis in mice, *Veterinary Research* 43 (2012) 62.
- [6] K. Debache, C. Guionaud, F. Alaeddine, M. Mevissen, A. Hemphill, Vaccination of mice with recombinant NcROP2 antigen reduces mortality and cerebral infection in mice infected with *Neospora caninum* tachyzoites, *International Journal for Parasitology* 38 (2008) 1455–1463.
- [7] D.K. Howe, A.C. Crawford, D. Lindsay, L.D. Sibley, The p29 and p35 immunodominant antigens of *Neospora caninum* tachyzoites are homologous to the family of surface antigens of *Toxoplasma gondii*, *Infection and Immunity* 66 (1998) 5322–5328.
- [8] J. Hiasa, J. Kohara, M. Nishimura, X. Xuan, H. Tokimitsu, Y. Nishikawa, ELISAs based on rNcGRA7 and rNcSAG1 antigens as an indicator of *Neospora caninum* activation, *Veterinary Parasitology* 187 (2012) 379–385.
- [9] J.S. Hoane, M.R. Yeargan, S. Stamper, W.J. Saville, J.K. Morrow, D.S. Lindsay, D.K. Howe, Recombinant NcSAG1 ELISA: a sensitive and specific assay for detecting antibodies against *Neospora hughesi* in equine serum, *Journal of Parasitology* 91 (2005) 446–452.
- [10] H. Zhou, J. Lee, T.J. Park, S.J. Lee, J.Y. Park, J. Lee, Ultrasensitive DNA monitoring by Au-Fe₃O₄ nanocomplex, *Sensors and Actuators B: Chemical* 163 (2012) 224–232.
- [11] A.M. Edwards, C.H. Arrowsmith, D. Christendat, A. Dharamsi, J.D. Friesen, J.F. Greenblatt, M. Vedadi, Protein production: feeding the crystallographers and NMR spectroscopists, *Nature Structural Biology* 7 (2000) 970–972.
- [12] S. Maeda, T. Kawai, M. Obinata, H. Fujiwara, T. Horiuchi, Y. Saeki, Y. Sato, M. Furusawa, Production of human α -interferon in silkworm using a baculovirus vector, *Nature* 315 (1985) 592–594.
- [13] E.Y. Park, T. Abe, T. Kato, Improved expression of fusion protein using a cysteine-, protease- and chitinase-deficient *Bombyx mori* (silkworm) multiple nucleopolyhedrovirus bacmid in silkworm larvae, *Biotechnology and Applied Biochemistry* 49 (2008) 135–140.
- [14] J. Wang, Nanomaterial-based amplified transduction of biomolecular interactions, *Small* 1 (2005) 1036–1043.
- [15] N.R. Jana, J.Y. Ying, Synthesis of functionalized Au nanoparticles for protein detection, *Advanced Materials* 20 (2008) 430–434.
- [16] P. Anger, P. Bharadwaj, L. Novotny, Enhancement and quenching of single-molecule fluorescence, *Physical Review Letters* 96 (2006) 113002.
- [17] K.H. Drexhage, Influence of a dielectric interface on fluorescence decay time, *Journal of Luminescence* 1–2 (1970) 693–701.
- [18] F. Tam, G.P. Goodrich, B.R. Johnson, N.J. Halas, Plasmonic enhancement of molecular fluorescence, *Nano Letters* 7 (2007) 496–501.
- [19] R. Bardhan, N.K. Grady, N.J. Halas, Nanoscale control of near-infrared fluorescence enhancement using Au nanoshells, *Small* 4 (2008) 1716–1722.
- [20] J.J. Mock, D.R. Smith, S. Schultz, Local refractive index dependence of plasmon resonance spectra from individual nanoparticles, *Nano Letters* 3 (2003) 485–491.
- [21] J.R. Lakowicz, Radiative decay engineering 5: metal-enhanced fluorescence and plasmon emission, *Analytical Biochemistry* 337 (2005) 171–194.
- [22] O. Ciftja, *Quantum Dots: Applications, Synthesis, and Characterization*, Nova Science Pub Incorporated, 2012.
- [23] P.R. Leroueil, S.A. Berry, K. Duthie, G. Han, V.M. Rotello, D.Q. McNerny, J.R. Baker Jr., B.G. Orr, M.M.B. Holl, Wide varieties of cationic nanoparticles induce defects in supported lipid bilayers, *Nano Letters* 8 (2008) 420–424.
- [24] E. Oh, M.Y. Hong, D. Lee, S.H. Nam, H.C. Yoon, H.S. Kim, Inhibition assay of biomolecules based on fluorescence resonance energy transfer (FRET) between quantum dots and gold nanoparticles, *Journal of the American Chemical Society* 127 (2005) 3270–3271.
- [25] J.N. Anker, W.P. Hall, O. Lyandres, N.C. Shah, J. Zhao, R.P. Van Duyne, Biosensing with plasmonic nanosensors, *Nature Materials* 7 (2008) 442–453.
- [26] J. Xie, Q. Zhang, J.Y. Lee, D.I.C. Wang, The synthesis of SERS-active gold nanoflower tags for in vivo applications, *ACS Nano* 2 (2008) 2473–2480.
- [27] M. Kodaka, Reply to the comment on reevaluation in interpretation of hydrophobicity by scaled particle theory, *The Journal of Physical Chemistry B* 106 (2002) 7717.
- [28] J. Dong, T. Otsuki, T. Kato, E.Y. Park, Development of a diagnostic method for neosporosis in cattle using recombinant *Neospora caninum* proteins, *BMC Biotechnology* 12 (2012) 19.
- [29] T. Otsuki, J. Dong, T. Kato, E.Y. Park, Expression, purification and antigenicity of *Neospora caninum*-antigens using silkworm larvae targeting for subunit vaccines, *Veterinary Parasitology* 192 (2013) 284–287.
- [30] X. Huang, Z. Zhao, J. Fan, Y. Tan, N. Zheng, Amine-assisted synthesis of concave polyhedral platinum nanocrystals having {4 1 1} high-index facets, *Journal of the American Chemical Society* 133 (2011) 4718–4721.
- [31] A.R. Tao, S. Habas, P. Yang, Shape control of colloidal metal nanocrystals, *Small* 4 (2008) 310–325.
- [32] E. Hao, R.C. Bailey, G.C. Schatz, J.T. Hupp, S. Li, Synthesis and optical properties of branched gold nanocrystals, *Nano Letters* 4 (2004) 327–330.
- [33] Y.G. Wang, S.P. Lau, X.H. Zhang, H.H. Hng, H.W. Lee, S.F. Yu, B.K. Tay, Enhancement of near-band-edge photoluminescence from ZnO films by face-to-face annealing, *Journal of Crystal Growth* 259 (2003) 335–342.
- [34] A. Hemphill, R. Felleisen, B. Connolly, B. Gottstein, B. Hentrich, N. Muller, Characterization of a cDNA-clone encoding Nc-p43, a major *Neospora caninum* tachyzoite surface protein, *Parasitology* 115 (1997) 581–590.
- [35] A. Hemphill, Subcellular localization and functional characterization of Nc-p43, a major *Neospora caninum* tachyzoite surface protein, *Infection and Immunity* 64 (1996) 4279–4287.
- [36] A. Hemphill, B. Gottstein, Identification of a major surface protein on *Neospora caninum* tachyzoites, *Parasitology Research* 82 (1996) 497–504.
- [37] N. Ban, C. Escobar, R. Garcia, K. Hasel, J. Day, A. Greenwood, A. McPherson, Crystal structure of an idiotype-anti-idiotype Fab complex, *Proceedings of the National Academy of Sciences of the United States of America* 91 (1994) 1604.
- [38] R. Bardhan, N.K. Grady, J.R. Cole, A. Joshi, N.J. Halas, Fluorescence enhancement by Au nanostructures: nanoshells and nanorods, *ACS Nano* 3 (2009) 744–752.
- [39] J. Lee, A.O. Govorov, J. Dulka, N.A. Kotov, Bioconjugates of CdTe nanowires and Au nanoparticles: plasmon-exciton interactions, luminescence enhancement, and collective effects, *Nano Letters* 4 (2004) 2323–2330.

Biographies

Hongjian Zhou received his BS degree in chemistry in 2007 from Nanyang Institute of Technology, China, and MS degree in materials physics and chemistry in 2010 from Jiangsu University of Science and Technology, China. Mr. Zhou is studying for his PhD degree in nano fusion technology from Pusan National University. His current research interest includes synthesis of multi-functional nanoparticles and biosensor applications. He is also interested in surface modification of nanocomposites for biocompatibility and biodegradability in bionano-medical applications.

Jinhua Dong is currently Assistant Professor in Shizuoka University, Graduate School of Science and Technology, Japan. He received his PhD degree in bioresources science from Graduate School of Bioresources, Mie University in 2007, and then worked as a Research Fellow in The University of Tokyo, Japan for 4 years. Dr. Dong is currently interested in antibody engineering by using phage display technology. Also he is interested in biosensor development and antibody therapeutics.

Vipin Kumar Deo is currently an Assistant Professor in Shizuoka University, Graduate School of Science and Technology. He received his BSc degree in chemistry from Bombay University, India in 1997, and MSc in biotechnology from Indian Institute of Technology-Bombay, India in 2000. He finished his PhD degree from Shizuoka University, Japan in 2006, and worked as Post-Doctoral Research scientist in University of Wyoming, USA for 1 year. Dr. Deo is currently interested in designing novel virus like particle based display system for protein expression and display for vaccination and drug delivery system using Silkworm expression system.

Enoch Y. Park is currently Professor in Integrated Bioscience Section, Graduate School of Science and Technology, Shizuoka University. He received his MS degree from Korea Advanced Institute of Science and Technology in 1982, and PhD degree in a major of chemical engineering from the University of Tokyo, Japan in 1990, and worked as Assistant Professor in Department of Chemical Engineering Nagoya

University for 2 years. Dr. Park is currently interested in preparation and engineering of nanobiomaterials such as virus-like particles. Also Dr. Park is interested in expression of eukaryotic proteins in silkworm larvae and their applicability on biological detection of molecules.

Jaebeom Lee is currently Associate Professor in Pusan National University. He received his PhD degree in chemistry from the Robert Gordon University, United

Kingdom in 2003, and worked as a Research Fellow in Chemical Engineering Department at the University of Michigan (UM), Ann Arbor till 2007. Dr. Lee is currently interested in fabrication and characterization of engineered assemblies of nanomaterials such as semiconductor materials and metallic materials and their biomedical applications.